Deliverable 2.1

Quality control methods for MEA and BP plate production

Author: VTT Technical Research Centre of Finland

Deliverable due date: 30.6.2021

Deliverable submission date: 8.7.2021

Dissemination Level		
PU	Public	x
PP	Restricted to other programme participants (including the Commission Services)	
RE	Restricted to a group specified by the consortium (including the Commission Services)	
CO	Confidential, only for members of the consortium (including the Commission Services)	
CON	Confidential, only for members of the Consortium	

This project has received funding from the Fuel Cells and Hydrogen 2 Joint Undertaking under Grant Agreement No 875081. This Joint Undertaking receives support from the European Union's Horizon 2020 Research and Innovation programme, Hydrogen Europe and Hydrogen Europe Research.

Table of Contents

1 Introduction

1.1 Summary of project scope

The objective of the project is to develop and demonstrate a compact and highly efficient micro combined heat and power (CHP) system based on high-temperature proton exchange membrane fuel cell (HT-PEMFC) technology and a novel two-stage methanol reformer consisting of a aqueous phase reformer and a steam reformer. The developed micro-CHP system is intended as a back-up solution for sequential or simultaneous cogeneration of electricity and thermal energy in rural areas with unstable or zero grid availability. A core focus on thermal integration and waste-heat recovery enable high fuel utilization, high electrical- and CHP efficiency, and dynamic load response and fast start-up for flexible integration with intermittent renewable energy sources. The main project goals and expected impacts are summarized below.

Table 1 – Expected project impacts and KPIs

Expected impact	KPI
Decrease system cost for small-scale CHP	CAPEX < 3000 €/kW
Decrease system size	System volume power density 30 W/L
Increase system lifetime	Degradation < 0.4 % / 1000h
Increased system efficiency	System electric efficiency > 50%
Fuel processor efficiency at BoL	> 85% fuel processor efficiency at BoL
Proved scalability of system and components	Design study of 50 – 100kW system
Flexible operation and RES support	Start-up time < 10 minutes

1.2 Purpose of the document

This document describes potential quality control methods that can be used in MEA and BP plate production. The improved quality control will help minimise flow resistance variation in stacks allowing higher fuel utilisation. Traditional and novel tools such as Artificial Intelligence (AI), and Machine vision for quality control are introduced and initial experiments for defect detection are reported.

2 Optical quality control

Machine vision is one of the key enabling technologies in intelligent manufacturing and has become the core component of automated optical inspection (AOI). By leveraging the latest advancements in sensor capabilities and breakthroughs in image processing algorithms, machine vision can greatly improve the efficiency of production lines, increase the level of automation, and minimize bottlenecks. Due to its non-contact and non-destructive properties, it represents the best approach for performing quality control inspections.

As illustrated in Figure 1, there are two main components for a defect detection machine vision system: imaging setup and image processing and defect detection software. The imaging setup is composed of two important subcomponents: optical illumination and imaging device. To be able to capture relevant features for defect detection, it is crucial to choose a combination of illumination and optics that would yield high-quality images.

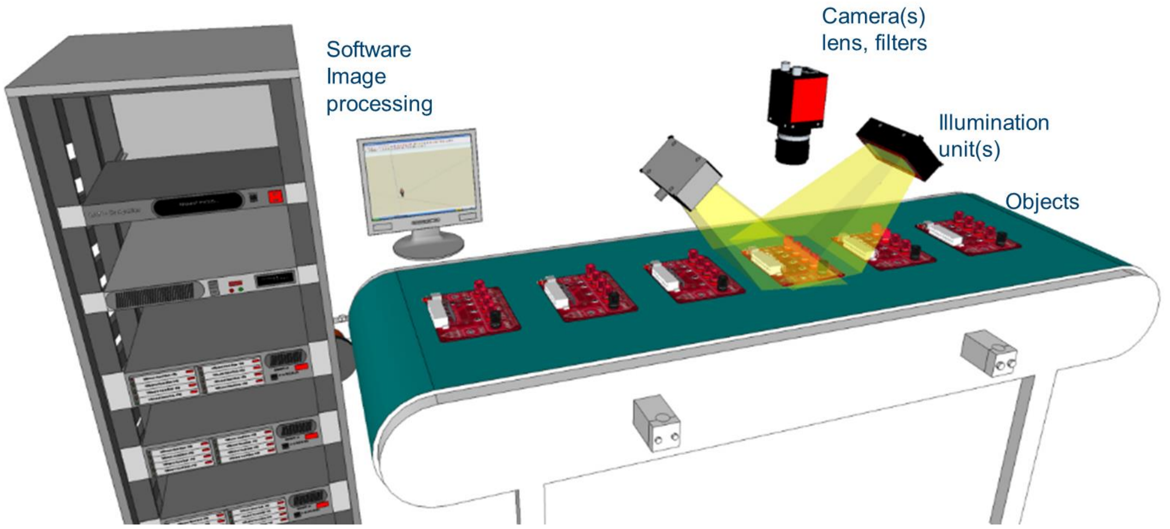

Figure 1. Illustration of a machine vision system.

Selection of optimal illumination and imaging method is determined by the requirements of quality measurement. Typical factors affecting the choices include:

- Material surface properties: color, glossy, matte etc.
- Required spatial resolution: size of defects that need to be detected
- Pass time: time allowed for measuring
- 3D shape: shape of the object that needs to be analyzed
- Measurement environment: conveyor belt, directly from process

In this deliverable, quality control of bipolar plate (BP) and membrane electrode assembly (MEA) is considered. The focus is on quality control of BP, which is more complex, whereas quality control of MEA is more directly approached using XRT.

3 Imaging

3.1 Illumination

The optical illumination plays a major role in highlighting different types of defects. Different illumination patterns can be selected based on the measurement requirement. Some typical illumination patterns are illustrated in Figure 2.

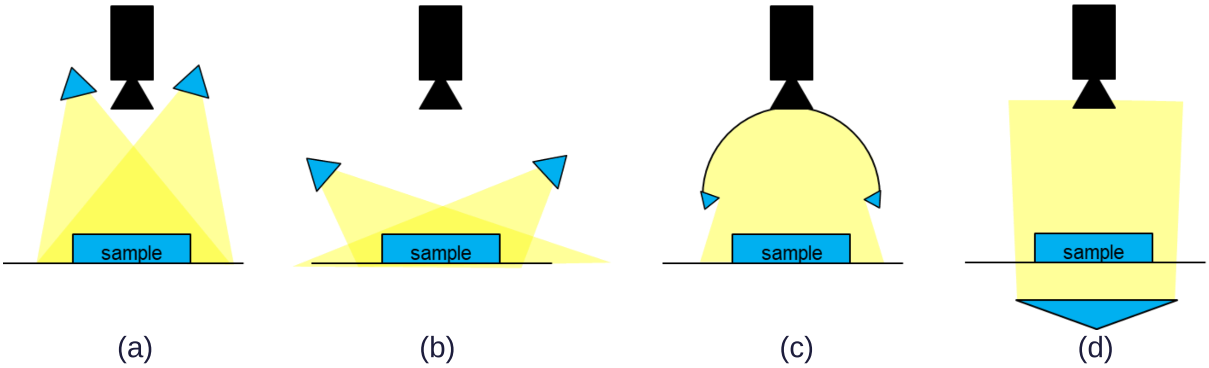

Figure 2. Illustration of typical illumination patterns. (a) Bright field illumination (b) Dark field illumination (c) Diffuse/dome illumination (d) Back illumination.

Depending on the incident angle of the lights, forward illumination can be divided in three main categories: bright-field, dark-field and diffuse illumination. A low angle-dark field forward lighting enhances structural defects, but it is prone to shadowing artifacts and obscures the texture of the material. Consequently, bright field imaging offers more texture information, but structural defects may be harder to emphasize. Diffuse lighting offers uniform illumination, which is more suitable for inspecting reflective, curved surfaces. Back illumination is used to capture the internal structure of a transparent or semitransparent object.

3.2 2D imaging

The two main camera types for 2D imaging are matrix camera and line scan camera. Matrix cameras are normal cameras that directly produce a 2D image. Typical industrial cameras reach up to 24MP resolution leading to roughly 20 µm pixel size in the object when short side of the BP plate is fully captured. Recently 40MP cameras have been introduced to market but despite almost doubling the pixel count, the size of pixel in object only decreases to roughly 15 µm. It should be noted that multiple images would need to be taken to cover the whole object or alternatively optics with a wider field of view should be used increasing the pixel size on object.

An alternative to matrix camera would be to use a line scan camera. Line scan camera captures a line of pixels instead of a full image. When object moves under the camera, multiple lines can be combined to a full 2D image. Line scan cameras are available with up to 16.000 pixels on a line [1], resulting in 7µm pixel size. Another benefit of line scan camera is easier illumination geometry control. The main drawback of line scan camera is the need for very accurate linear movement of object whereas matrix camera can capture the spatial information directly.

3.3 3D imaging

Line scanning or laser profilometry is one of the earliest 3D imaging methods. The core idea behind this concept is simple; a laser line is projected onto the target object, which is imaged with a different angle.

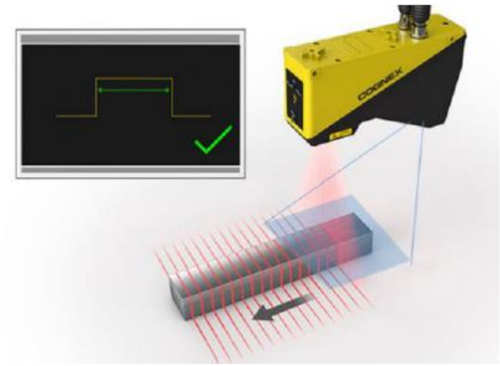

Figure 3 Line scanning principle [2]

Any 3D shape differences shift the line in the image and the 3D profile can be computed using triangulation. Similar to a line scan camera, a 3D image/surface is acquired by scanning consecutive profiles, which offers information about the shape of the object. Using this imaging method, it is easy to identify defects in the shape of the object by analysing the depth variance. One important assumption is that the object's surface is not fully reflective/glossy or transparent, otherwise the measurements are not correct.

Structured light technique can be considered as a spatial extension of line scanning, where instead of a line, a full picture is projected onto the measured surface. The 3D target object will deform the lines and using triangulation/trigonometry, the 3D profile can be computed and used to check if the object surface corresponds to the quality standards. Compared to laser profilometry, it can acquire the 3D profile by taking only one snapshot instead of multiple line scans. Again, defects in the shape of objects can be detected by investigating the obtained 3D profile and picking up any deviation in terms of depth.

It should be noted that there is a trade-off between the width of the measurement line and z-resolution. When measuring a larger object with a wider line, the depth measurement accuracy becomes lower.

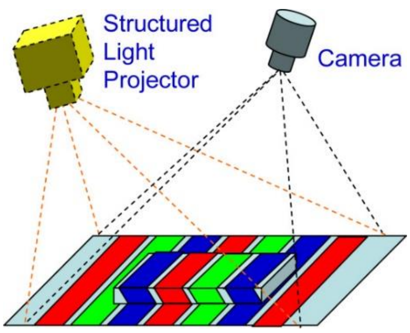

Figure 4 Structured light principle.

3.4 X-ray imaging

For transparent objects, back illumination may be used to measure through the objects. However, often this is not possible, as light cannot pass through the measured objects. In this scenario, an alternative to optical measurement is to use X-ray transmission imaging (XRT) where an X-ray source irradiates the sample and penetrated X-rays are captured by X-ray imaging detector. Recently, high-resolution Medipix3 hybrid pixel detectors [3] have been developed that offer 55 µm pixel size and imaging of two energy ranges simultaneously.

The quality control of MEA focuses on material homogeneity. The natural way to approach this analysis need is to use XRT technology.

4 Data analysis

With the proliferation of modern imaging techniques, the ability to analyze the produced image data must adapt to the strict requirements of quality control in industrial environments. To ensure almost perfect accuracy at high speeds, data needs to be analyzed in an efficient manner. For this, machine vision systems have successfully utilized traditional image processing and pattern recognition techniques for decades. Relying on manually tuned feature extractors and hand-designed rules built by computer vision engineers, the system can then automatically inspect the target and decide if it adheres to the quality standards or not. These techniques proved to be very efficient and many systems are still relying on them nowadays due to their increased reliability and resilience to fatigue as opposed to human visual inspection, which has clear limitations. However, in light of Industry 4.0 and today's recent advancements in optical technology, the amount of available data has increased exponentially, posing a challenge to established methods in terms of efficiently and correctly analyzing this data. A new breed of algorithms has emerged in Computer Vision, which addresses the problem of processing huge amounts of data while maintaining and even exceeding accuracy and robustness standards. These algorithms come under the umbrella of Machine Learning (ML) and focus on building classifiers that can learn patterns and rules from the provided data. Neural networks are momentarily the biggest trend in ML and Computer Vision, being utilized in a wide range of vision-related problems.

4.1 Traditional methods

Traditional image processing and pattern recognition algorithms were the founding blocks of image-based analysis. Some of these algorithms are still being successfully used in our days, mainly for problems that can be suitably constrained, for example in the case of quality control, if objects of interest are of known shape and texture, then it is easy to filter them if the corresponding shape or material is different. Typical image processing algorithms are built by combining methods such as filtering, thresholding, grayscale transformation, edge detection, blob detection, template matching, etc. in a sequential pipeline, for emphasizing potential defects. In [4], a revised method of Otsu method for thresholding is applied automatic selection of optimal threshold value for defect detection in applications like contamination inspection or surface scratch. Spectral approaches operate on images in a transformed domain, where various filters are applied, like Fourier transforms, wavelet transforms or Gabor transforms. Tsai and Huang [5] applied Fast Fourier Transform (FFT) for detecting local defects embedded in statistical textures. Similarly, Gabor transform is a type of windowed FT, where the windowed function is a Gaussian. The work of [6] provides a comparison between an improved gray level co-occurrence (GLCM) implementation and a Gabor filter based approach for detecting fabric defects. For the Gabor approach, the authors are using a combination of even and odd symmetric Gabor filter for detecting both blob-shaped and edge-shaped fabric defects. However, their GLCM method yielded higher detection accuracy and computational efficiency than the Gabor approach, in the same environment.

Conventional pattern recognition methods are relying on complex feature extractors designed by engineers, to compress the amount of data and improve the detection efficiency. The extracted features are then utilized in the training process of classifiers, which will be able to classify and predict the defects in newly acquired images. The most representative classifiers for supervised pattern recognition are SVM and kNN classifiers. To obtain GLCM features, the authors of [7] preprocessed the images using a pipeline of wavelet, threshold and morphological operations. Then, defective images are classified using the kNN algorithm. All operations were performed on images taken from a thermal camera, with the scope of detecting fabric defects. Xie and Mirmehdi [8] proposed generating texture exemplars (TEXEMS) and based on Gaussian mixture model, obtain the distribution of color textures which is used in defect detection on ceramic tiles. X. Zhou et al. [9] designed an automated visual apparatus for bottle bottom inspection, utilizing saliency detection and template matching. Another type of feature descriptors are histograms of oriented gradients (HOG), that have been successfully applied in anomaly detection for wire ropes [10] or patterned fabric [11]. To extract HOG descriptors, gradients images are computed and the image is divided in cells, for which gradient orientation histograms are calculated.

The challenge with these image processing-based approaches is that each step in the pipeline usually has some parameters that need to be tuned and modifying each parameter may cause further parameter refinement in subsequent steps as well. Moreover, when fine tuning the parameters, one must take in consideration possible disturbances in the operating environment and design a sufficiently robust solution. This can lead to maintaining an impracticable huge amount parameter space. In addition, as the manufacturing processes are refining more and more, the nature of defects is more complex and detecting them requires better performing algorithms.

4.2 Machine learning

The Computer Vision community has recently seen a great increase in the utilization of Machine Learning techniques. Particularly, methods based on neural networks and deep neural networks are proving to be more robust, accurate and efficient, outperforming earlier methods especially in difficult tasks such as object detection and semantic or instance segmentation. A visual understanding of these problems is depicted in Figure 5

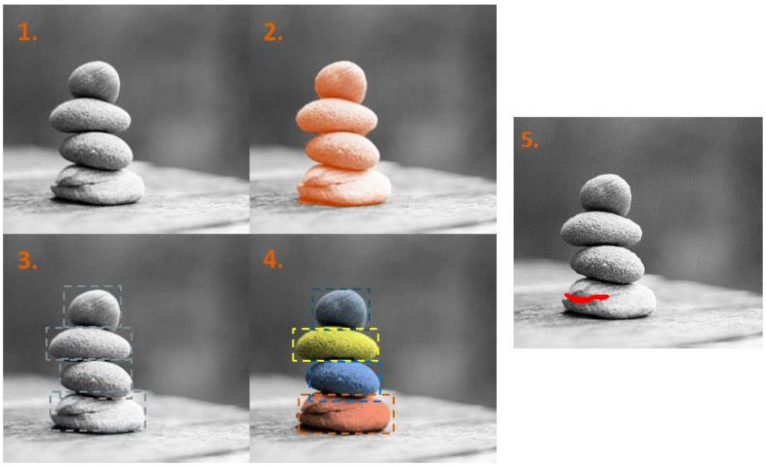

Figure 5. Types of Computer Vision problems

There are two main approaches for solving these problems: supervised and unsupervised learning. In supervised learning, a neural network is trained for detecting the anomalies by providing labelled training data. Practically, someone needs to manually annotate the possible defects and flaws, either on image or pixel level and then feed the data to the neural network. By having examples of how defects might look like, the neural network learns the necessary patterns of these anomalies and is able to detect them in newly acquired images. The network can be designed for any of the tasks mentioned above. The main bottleneck of supervised learning is obtaining and labelling the data. Even obtaining large amounts of data consisting of faulty defects is quite challenging, especially since the current manufacturing processes typically have a low ratio of defects, to which it adds the laborious process of annotating the data.

Hence, for some cases, it is better to apply unsupervised learning, which directly analyzes and clusters data and does not need associated labels. Therefore, the faults are not directly modeled, but they are regarded by the networks as outliers from the correct data. However, in practice, there is still a need for annotating data in order to validate the performance of the system, but the magnitude of annotated data is significantly reduced than in the case of supervised learning.

To get a better understanding of how ML can be applied in quality control applications, we briefly analyze each type of task, highlighting state-of-the-art implementations and how they are transferred to practical applications.

Image classification (1) was the first proposed problem, historically speaking, and it simply aims at solving the task of identifying the class of the image or of the main object present in the image, regardless of position, orientation, or other nearby objects. There is an assumption that only one class is assigned per image, representing the main depicted object. If the goal of the quality inspection is to either accept or discard objects, then employing an architecture designed for image classification is the most efficient way to proceed, due to their reduced complexity and fast inference time. Most of the time, the problem is formulated as a two-class binary problem, namely faulty or not faulty classes; images with objects that present defects have the faulty label assigned to them after classification, so that appropriate decisions can be taken after (discard or revise product). Popular architectures for Image Classification are AlexNet [12], VGGNet [13], DenseNet [14] or Inception-v4 [15]. The authors of [16] have successfully implemented a similar, simplified version of AlexNet architecture, capable of classifying mistakes occurring in the process of producing gravure cylinders, reaching a classification accuracy rate of 98.4%. Some inherent limitations of image classification are the inability of localizing defects in the image and working under the strict assumption of having exactly one instance of the target object.

Semantic segmentation (2) operates on a different principle and assigns classes to all pixels in an image. The major advantage of formulating the problem as a semantic segmentation task is the fine granularity of the output and the ability of dealing with multiple classes in the same image. State-of-the-art architectures designed for this task have gained momentum from Fully Convolutional Networks (FCN) [17] and are now represented by U-Net [18], DeepLabv3+ [19] or ParseNet [20]. Inspired by the results of these networks, the authors of [21] used a custom convolutional encoder-decoder architecture to segment defects in rolling element surface scans. Similarly, a symmetric convolutional neural network based on U-net described in [22] was utilizing for finding surface defects in mobile phone back glass, yielding an average precision of 91% and average recall of 95%. Although defects can be detected at fine granularity, semantic segmentation does not distinguish between multiple instances of the same class, and without post-processing, large defects could in fact, consist of multiple smaller and linked defects, which might be a problem, depending on the use case. Additionally, the task of labelling images for semantic segmentation is one of the most laborious one since it operates at pixel level.

Object detection (3) identifies and localizes multiple objects in the same image, enclosing them in bounding boxes. This enables the differentiation between multiple instances of the same object and simultaneously predicting the location of each instance in the image. These are appealing properties for advanced quality control systems since the locations of defects can be used in the revision process of the product. Significant breakthroughs in this task has been achieved by the following architectures: SSD [23], YOLO [24] and Faster R-CNN [25]. The authors of [26] have improved the original Faster R-CNN and utilized a Feature Pyramid Network (FPN) [27], for detecting six common types of PCB surface defects. The only drawback of using object detection is the limitation of bounding box approximations. For particular applications, bounding boxes may not offer consistent approximations, especially for elongated or irregular shaped objects.

Instance segmentation (4) builds on top of object detection and semantic segmentation by adding a segmentation mask for each detected instance, resulting in an accurate representation of the object and a precise localization in the image. The output of the network will predict enclosing bounding boxes as well as segmentation masks for all instances. Therefore, it is the most complex task to be solved. The flagship architecture in this task is Mask R-CNN [28], followed by more specialized architectures such as Yolact [29] (real-time capabilities) or PANet [30]. M. Ferguson et. al [12] successfully employed an architecture based on Mask R-

CNN to identify casting defects in X-ray images. Compared to the other tasks, although instance segmentation provides the most amount of information about defects, there is a natural increase in processing time and memory footprint. Recent architectures, like Yolact, already started to address these issues and offer reasonable tradeoffs between accuracy and speed.

Anomaly detection (5) aims at finding irregularities/anomalies in images that do not correspond to the desired output. It can be implemented in two ways: supervised and unsupervised learning. If supervised learning approach is employed, then anomalies (defects) must be manually annotated and then neural networks can be trained for any of the above-mentioned tasks to find the defects in images. However, due to the laborious task of annotating and rarity in defect occurrence, the best approach is to model anomaly detection as an unsupervised learning problem. In this case, anomalies are not modeled explicitly, but correct/accurate data is first modeled, so that any new sample is tested against this reference model and if there is a significant variance, it means that there must be an anomaly in the sample. This way, new kinds of anomalies can be detected, even if these types were not previously known. In [31], authors use a convolutional autoencoder architecture to detect defects in formed sheet metals, like wrinkles or cracks. Other known architectures for unsupervised anomaly detection are Deep Belief Networks [32]. However, to validate unsupervised learning algorithms, a labelled test dataset is still needed, such that the performance can be estimated.

The decision of choosing which type of neural network to employ and how to model the problem for realizing optical quality control depends on the nature and complexity of defects that are bound to happen in the operating environment and additionally, both the availability of data and the cost of labelling it.

5 Quality control in MEA and BP plate production

5.1 MEA

A Membrane-Electrode-Assembly (MEA) is what constitutes a cell in a fuel cell. In a Proton-Exchange-Membrane fuel cell (PEM-FC) the membrane is typically made of a special polymer film imbibed (or doped) with an electrolyte. The electrolyte will carry the protons (+) from single hydrogen atoms across the membrane and block the electrons (-) from passing the membrane. Charge has been separated and a cell voltage established. The current of the cell is proportional with the number of times this happens.

The typical “fuel” is a gas of hydrogen molecules (H2) either directly or a hydrogen-rich gas reformed from methanol. In both cases the problem is that the hydrogen is bound as a molecule (two atoms) and this molecule cannot be carried over by the electrolyte. The molecule must be reformed to single Hydrogen atoms by a platinum (Pt) catalyst dispersed on the Electrode. This is typically Pt nanoparticles placed on larger graphite spheres to increase the active Pt surface area.

Since the pure Pt metal is expensive and can constitute the main part of the value in a fuel cell stack, the quality of the electrode must be inspected. This is to look for non-uniform coatings and Pt-loading that is either too low (not enough catalytic activity) or too high (too expensive). Since all cells in a fuel cell stack are electrically in series, it is important that the catalytic reactivity is uniform so a weak link will not dominate the performance.

To inspect the quality of the electrode coating and x-ray image can be taken to inspect the Pt-loading. In Figure 1 an x-ray image of various Pt-loadings on square electrodes are shown together with a full MEA on the right side.

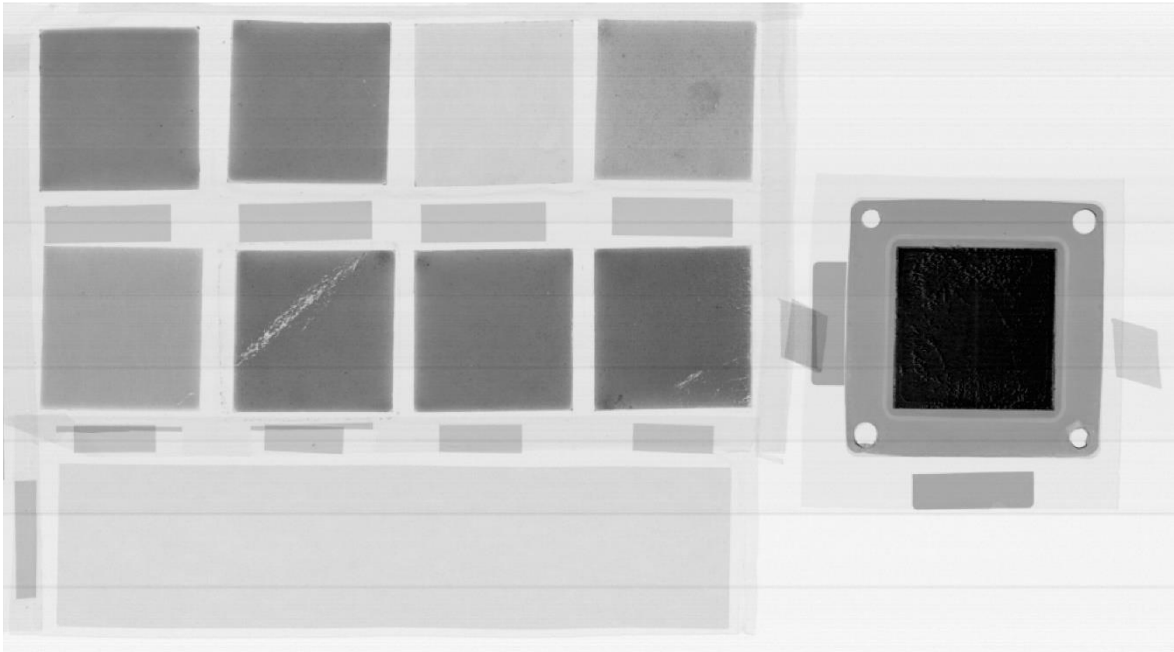

Figure 6. Illustration of Pt-loadings on square electrodes together with a full MEA

Both the uniformity and the overall intensity can be inspected and qualified since the Pt-loading of the square electrodes is already known.

At Blue World Technologies an inline x-ray machine is being incorporated in the electrode coating line in order to be able to directly feed back the Pt-loading values to the production line.

5.1 BP plates

This section describes various the tests conducted in VTT laboratory for analysing the BP plate defects. The experiments are based on BP samples that were sent to VTT by BWT. The samples included a small number of defective samples from production and good samples. For analysis purposes, defects were also manually introduced to some of the good samples.

The most typical defects in BPs were identified as:

1. Edge chips
2. Porosity on edge area
3. Dents of the channel ridges

These defects are illustrated in Figure 7

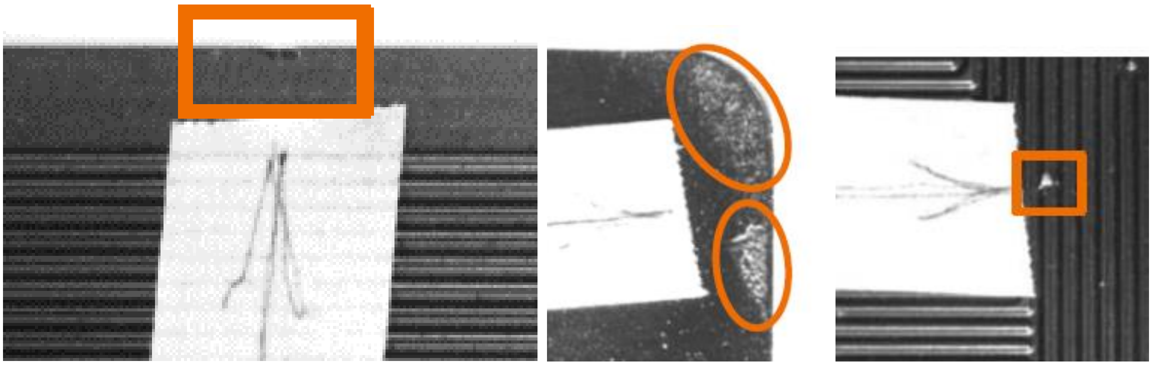

Figure 7. Illustration of defect types.

BP Imaging experimentation

As described in section 3.1, different illuminations can be used to highlight different properties of the objects being analysed. In the analysis of BP, bright field and dark field illumination were found useful. Figure 8 illustrates how different defect types respond to different illumination patterns. For example, porosity is easily observable using either bright field or dark field illumination compared to diffuse illumination. In addition, the missing part of material in the channel is well seen in the dark field illumination and much more difficult to see in the diffuse illumination. It should be noted that dark field illumination needs to be applied at least from two different directions separately to capture all defects.

The defects in the rides and edge chips of the plates can also be easily seen in 3D. Figure 9 illustrates a defect captured using a laser scan. However, utilizing the depth measurement to analyse the porosity is not as straight forward as the deviation from normal plate plane is rather small.

To understand the effect of defect size to the visual appearance in the 2D images, defects of different size were manually made to good plates. Figure 10 illustrates the appearance of defects in the dark field image and the measured 3D shape of defects. It should be noted that the applied 3D measurement method in this image is not practical for production use due to small measurement area but is used here to give an accurate reference.

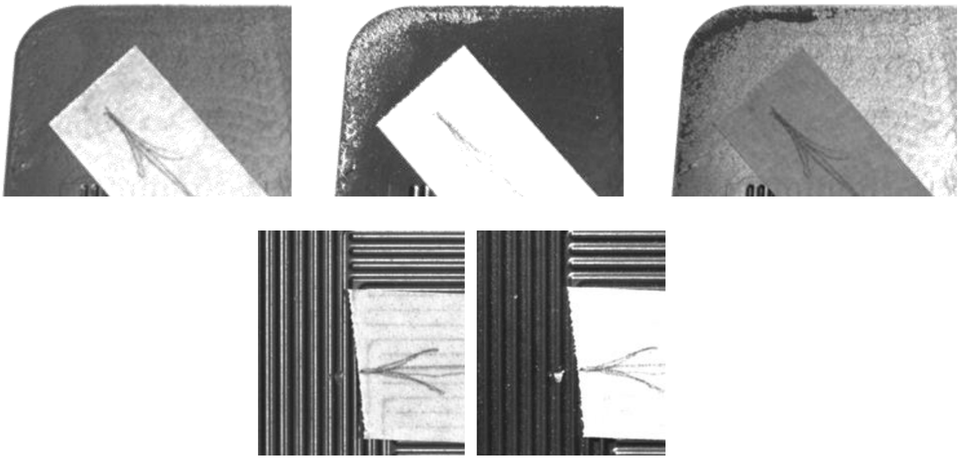

Figure 8. Illustration of the effect of different illumination patterns. Top: diffuse illumination, dark field illumination and bright field illumination. Bottom: diffuse illumination and dark field illumination

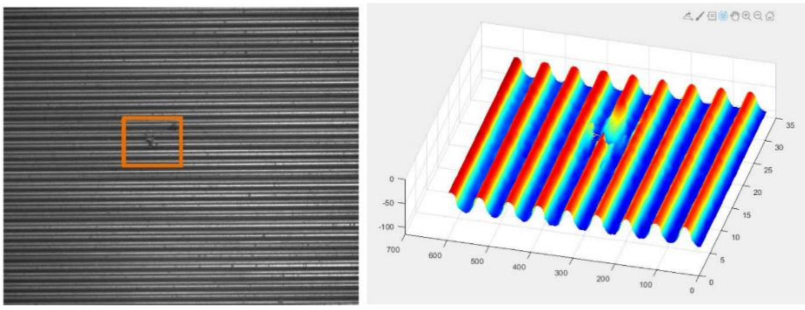

Figure 9. Illustration of a defect with diffuse lighting (left) and 3D measurement.

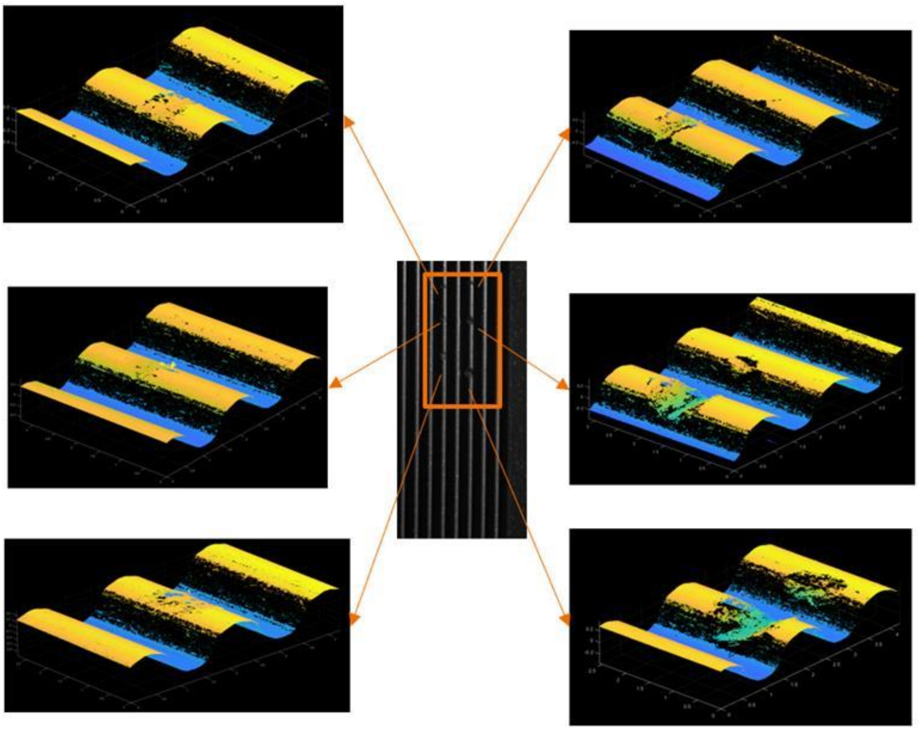

Figure 10. Illustration of appearance of defects in the dark field image and the measured 3D shape of defects.

Data analysis approaches

To highlight potential solutions for the task of finding defects from BP plates and to give an applied comparison between different methods, three data analysis approaches have been tested.

The most straightforward and conceptually simple method is image subtraction, or sometimes known as template matching. The main idea is to have a reference image of a plate with no defects, that is considered the ideal model. In the next step, new plates are imaged and compared to the reference model by performing image subtraction in intensity domain. Ideally, the reference and the target images are similar, and the subtracted image does not have any variation, meaning that there are no defects. If defects are present, then the subtracted image will have intensity variation at defects locations, highlighting both the location and the size. Image subtraction concept works on two major assumptions: same illumination conditions in reference and target images and perfect alignment of the objects of interest. The former requirement is easy to fulfill in this environment, as the light sources are static and there are no external factors to disturb the lightning conditions. For satisfying the latter requirement, an image registration algorithm is needed for aligning the reference plate with the target plates, due to small positioning deviations of the plates.

There are two approaches for realizing image registration: feature based and direct image alignment. Feature-based registration algorithms are extracting relevant, salient features from the images, such as SIFT, ORB, SURF, etc. Based on the extracted features, descriptors are calculated for each feature, which will be used in the feature matching phase, where features from the two images are matched. Ultimately, a transformation (affine, projective, Euclidean, etc.) can be estimated from the feature correspondences. However, feature extractors rely on textured areas to extract corners or blobs, but in this case, the surface of BP plates does not have strong textures, making it difficult to extract robust key points. Therefore, the next registration technique used was direct image alignment, where the transformation is estimated from the optimization of photometric error, hence exploiting all the information in images, even where the gradients are small. Some of the popular direct image alignment algorithms are dense optical flow [33] and phase cross correlation [34].

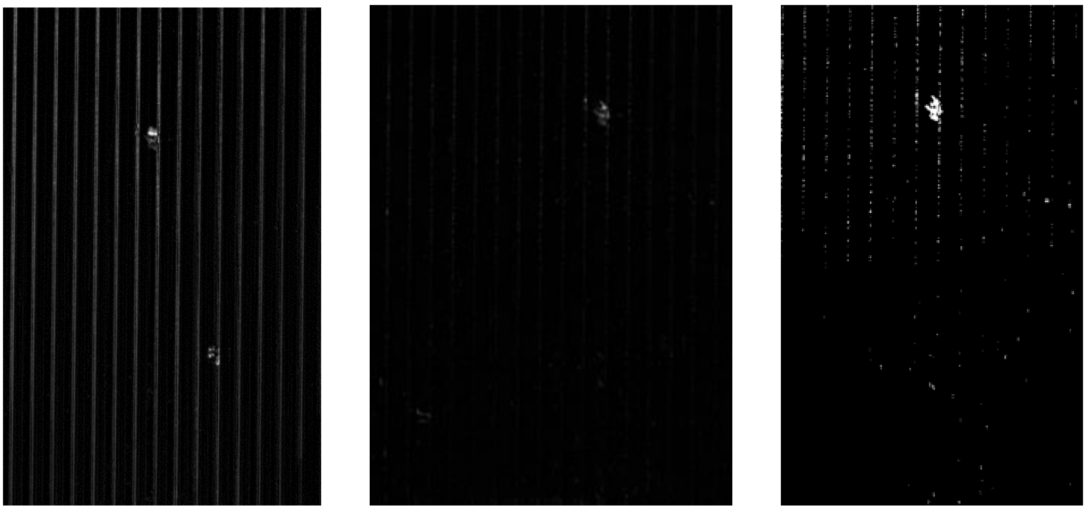

(a) (b) (c)

Figure 11. Image registration techniques: image difference using (a) cross correlation (b) optical flow (b). The obtained difference image can be thresholded and the result can be seen in (c).

The above results show that image alignment needs to be as accurate as possible to avoid false positives. Defects can be highlighted by using this technique, but because of the high intensity variation and narrow width of pattern features of the plate, exact alignment is very difficult to obtain, resulting in detection of false positive defects.

Due to the complexity of realizing exact image alignment, an alternative solution, robust to slight misalignment, consists in doing image difference based on HOG features. The image is divided in patches and HOG features are calculated for each patch. Using different distance metrics (L1 and L2 squared norm) the difference between the reference and target image can be calculated. Using the feature representation and image patches makes the method less reliable to small registration errors. Figure 12 illustrates the result of HOG feature based analysis.

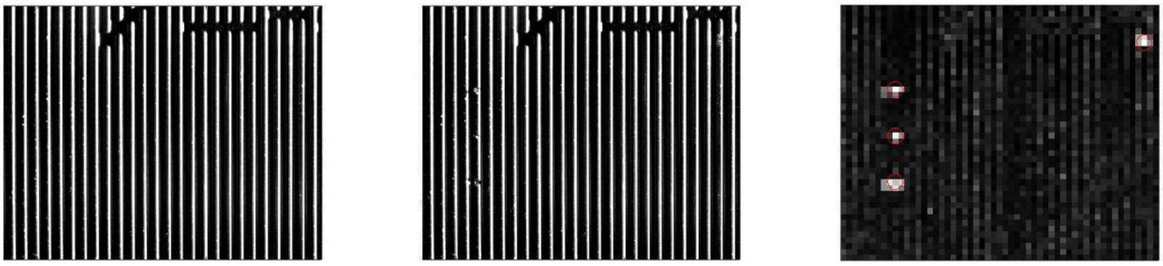

(a) (b) (c)

Figure 12. Illustration of (a) good sample (b) sample with defects (c) analysis based on HOG features.

All the above experiments rely on a fundamental step and that is exact image alignment, which proved to be difficult to achieve. Therefore, an ML-based method was implemented, leveraging the power of convolutional autoencoders.

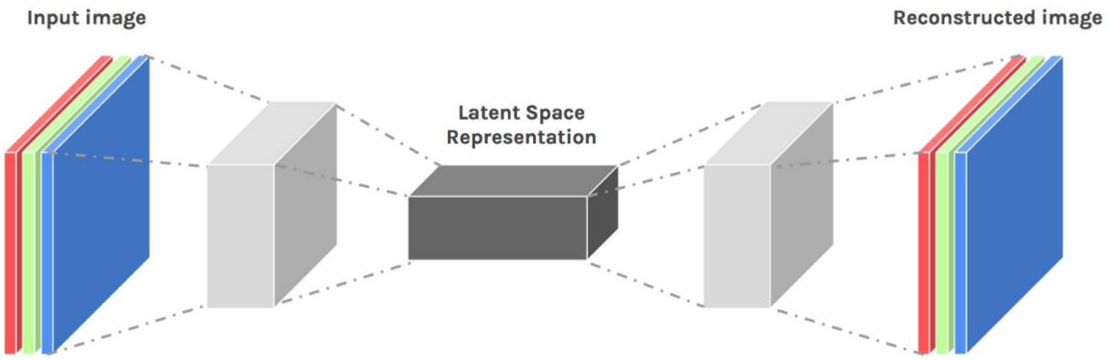

Figure 13 Autoencoder architecture.

Autoencoders are neural networks based on unsupervised learning. Given an input image, the autoencoder first encodes the image in a lower latent space representation and then decodes the representation back to an image. The goal of the autoencoder is to learn the latent representation which minimizes the reconstruction error. By providing reference images of plates without defects, the autoencoder will learn how to properly reconstruct the plates. When images of defective plates will be fed to the network in inference mode, the latent representation will be able to reconstruct the plate as close as possible to the input, but it will fail to reconstruct the defects. Having the input image with defects and the reconstruction consisting of what the “ideal” plate should look like; the two images can be subtracted, and defects will be highlighted. Because the reconstruction is based on the input image, this means that the images are by default aligned.

An experiment using the autoencoder neural network was performed with the dark field BP images. Figure 14 illustrates some input and reconstruction pairs. It can be seen that the concept works well for edge chips (a, b) and channel defects (c, d) where the defects are erased from the reconstruction. However, there are some more complex areas (e, f) where the reconstruction also fails for some real structures and would cause false defect detections.

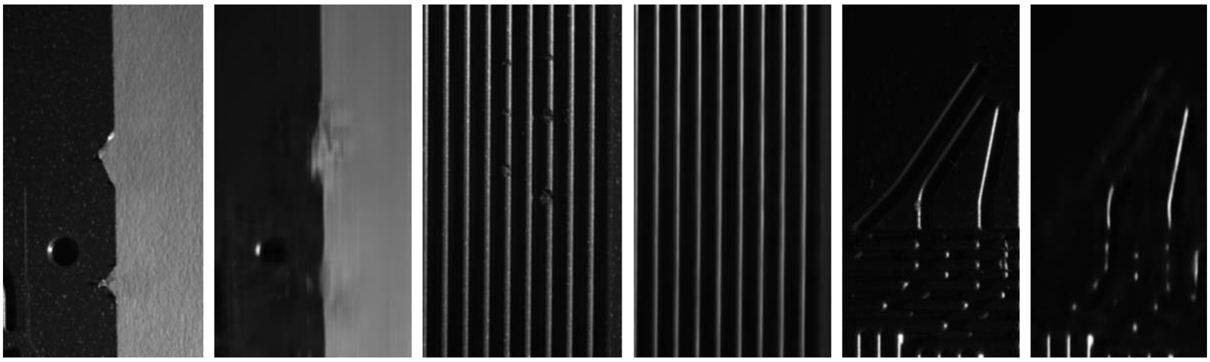

(a) (b) (c) (d) (e) (f)

Figure 14. (a,c,e) Input images to neural network and the resulting (b, d, f) reconstructed images

Summary and conclusions

Based on the research work done on the project, preliminary concept is proposed for the quality inspection of the BP plates. The concept is a machine vision system consisting of area imaging camera and applying multiple illumination geometries as illustrated in Figure 15. Plates could be imaged “at-line” on a conveyor belt in production, without specific inspection unit and manipulation of the plates.

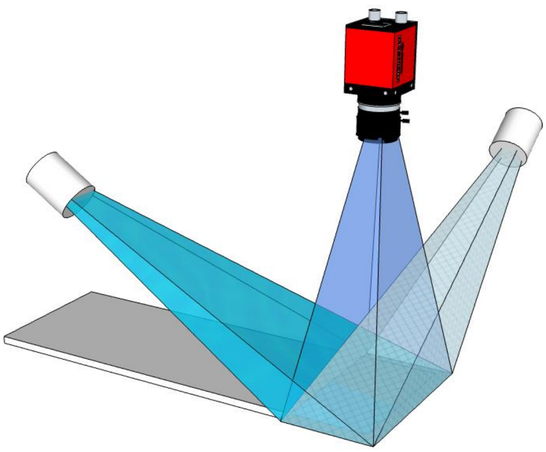

Figure 15. Concept illustration of x- and y-directed illumination and imaging of the plate.

Consecutive images are taken of the plates with e.g. x- and y-direction illumination, covering the whole are the plate. Two different approaches for analysis were considered: First, traditional machine vision methods and patter recognition could be applied by comparing the plates images to similar reference images, which do not contain any defects. The defects are revealed by the difference. Straightforward pixel-by-pixel difference of the images proved to be susceptible to image aligned and matching errors. For this reason, image feature matching using. e.g. HOG features, which are more tolerant to alignment, are proposed instead. As a second approach, AI methods could be used as anomaly detection, as explained earlier. Also another option considering structural 3D defects, 3D imaging could be used instead of normal camera. The porosity defects however require the traditional 2D camera with directed illumination.

Line camera option was also considered in the study. It has advances e.g. related to illumination homogeneity, but requires precise movement to provide undisturbed image, which could be susceptible to conveyor belt jitter in practice.

Bibliography

[1] [Online]. Available: https://www.teledynedalsa.com/en/products/imaging/cameras/linea/. [Accessed 30 6 2021].

[2] "Gognex," [Online]. Available: https://www.cognex.com/products/machine-vision/3d-machine-vision-systems/in-sight-laser-profiler.

[3] R. Ballabriga, M. Campbell, E. Heijne, X. Llopart, L. Tlustos and W. Wong, "Medipix3: A 64k pixel detector readout chip working in single photon counting mode with improved spectrometric performance," *Nucl. Instrum. Methods Phys. Res. A,* vol. 633, pp. S15-S18, 2011.

[4] H.-F. Ng, "Automatic thresholding for defect detection," in *Third International Conference on Image and Graphics (ICIG'04)*, 2004.

[5] D.-M. Tsai and T.-Y. Huang, "Automated surface inspection for statistical textures," *Image and Vision Computing,* vol. 21, no. 4, pp. 307-323, 2003.

[6] J. L. Raheja, S. Kumar and A. Chaudhary, "Fabric defect detection based on GLCM and Gabor filter: A comparison," *Optik,* vol. 124, no. 23, pp. 6469-6474, 2013.

[7] K. Yıldız, A. Buldu and M. Demetgul, "A thermal-based defect classification method in textile fabrics with K-nearest neighbor algorithm," *Journal of Industrial Textiles,* vol. 45, no. 5, p. 780–795, 2016.

[8] X. Xie and M. Mirmehdi, "TEXEMS: Texture exemplars for defect detection on random textured surfaces," *IEEE Transactions on Pattern Analysis and Machine Intelligence,* vol. 29, no. 8, pp. 1454-1464, 2007.

[9] X. Z. e. al., "Automated Visual Inspection of Glass Bottle Bottom With Saliency Detection and Template Matching," *IEEE Transactions on Instrumentation and Measurement,* vol. 68, no. 11, pp. 4253-4267, 2019.

[10] C. Li, G. Gao, Z. Liu, D. Huang and J. Xi, "Defect Detection for Patterned Fabric Images Based on GHOG and Low-Rank Decomposition," *IEEE Access,* vol. 7, pp. 83962-83973, 2019.

[11] P. Esther-Sabrina, "On the Suitability of Different Features for Anomaly Detection in Wire Ropes," *Computer Vision, Imaging and Computer Graphics. Theory and Applications,* pp. 296--308, 2010.

[12] A. Krizhevsky, I. Sutskever and a. G. E. Hinton, "In Proceedings of the 25th International Conference on Neural Information Processing Systems," in *25th International Conference on Neural Information Processing Systems*, Red Hook, NY, USA, 2012.

[13] S. Liu and W. Deng, "Very deep convolutional neural network based image classification using small training sample size," in *2015 3rd IAPR Asian Conference on Pattern Recognition (ACPR)*, 2015.

[14] G. Huang, Z. Liu, L. V. D. Maaten and K. Q. Weinberger, "Densely Connected Convolutional Networks," in *2017 IEEE Conference on Computer Vision and Pattern Recognition (CVPR)*, 2017.

[15] C. Szegedy, S. Ioffe, V. Vanhoucke and A. A. Alemi, "Inception-v4, inception-ResNet and the impact of residual connections on learning," in *In Proceedings of the Thirty-First AAAI Conference on Artificial Intelligence (AAAI'17)*, 2017.

[16] J. S. D. G. R. O.-M. J. B. M. &. W. W. Villalba-Diez, "Deep Learning for Industrial Computer Vision Quality Control in the Printing Industry 4.0," *Sensors (Basel, Switzerland),* vol. 19(18), p. 3987, 2019.

[17] J. Long, E. Shelhamer and T. Darrell, "Fully convolutional networks for semantic segmentation," in *2015 IEEE Conference on Computer Vision and Pattern Recognition (CVPR)*, 2015.

[18] O. Ronneberger, P. Fischer and T. Brox, "U-Net: Convolutional Networks for Biomedical Image Segmentation," in *Medical Image Computing and Computer-Assisted Intervention – MICCAI 2015*, 2015.

[19] L.-C. Chen, Y. Zhu, G. Papandreou, F. Schroff and H. Adam, "Encoder-Decoder with Atrous Separable Convolution for Semantic Image Segmentation," in *ECCV*, 2018.

[20] W. Liu, A. Rabinovich and A. C. Berg, "ParseNet: Looking Wider to See Better," in *CoRR*, 2015.

[21] B. M. B. G. D. F. L. A. Prappacher N, "Defect Detection on Rolling Element Surface Scans Using Neural Image Segmentation," *Applied Sciences,* vol. 10, p. 3290, 2020.

[22] J. J, C. P, L. Z, L. W and Y. Y, "Surface Defect Detection for Mobile Phone Back Glass Based on Symmetric Convolutional Neural Network Deep Learning," *Applied Sciences,* vol. 10, p. 3621, 2020.

[23] W. Liu, D. Anguelov, D. Erhan, C. Szegedy, S. Reed, C.-Y. Fu and A. Berg, "SSD: Single Shot MultiBox Detector," in *European Conference on Computer Vision*, 2016.

[24] J. Redmon, S. Divvala, R. Girshick and A. Farhadi, "You Only Look Once: Unified, Real-Time Object Detection," in *IEEE Conference on Computer Vision and Pattern Recognition (CVPR), 2016*, 2016.

[25] S. Ren, K. He, R. Girshick and J. Sun, "Faster R-CNN: Towards Real-Time Object Detection with Region Proposal Networks," *IEEE Transactions on Pattern Analysis and Machine Intelligence,* vol. 39, pp. 1137-1149, 2017.

[26] B. Hu and J. Wang, "Detection of PCB Surface Defects With Improved Faster-RCNN and Feature Pyramid Network," *IEEE Access,* vol. 8, pp. 108335-108345, 2020.

[27] T. Lin, P. Dollár, R. Girshick, K. He, B. Hariharan and S. Belongie, "Feature Pyramid Networks for Object Detection," in *017 IEEE Conference on Computer Vision and Pattern Recognition (CVPR)*, 2017.

[28] K. He, G. Gkioxari, P. Dollár and R. Girshick, "Mask R-CNN," in *2017 IEEE International Conference on Computer Vision (ICCV)*, 2017.

[29] D. Bolya, C. Zhou, F. Xiao and Y. J. Lee, "YOLACT: Real-Time Instance Segmentation," in *2019 IEEE/CVF International Conference on Computer Vision (ICCV)*, 2019.

[30] S. Liu, L. Qi, H. Qin, J. Shi and J. Jia, "Path Aggregation Network for Instance Segmentation," in *2018 IEEE/CVF Conference on Computer Vision and Pattern Recognition*, 2018.

[31] J. Heger, G. Desai and M. Z. E. Abdine, "Anomaly detection in formed sheet metals using convolutional autoencoders,," *Procedia CIRP,* vol. 93, pp. 1281-1285, 2020.

[32] J. Sun, A. Steinecker and P. Glocker, "Application of Deep Belief Networks for Precision Mechanism Quality Inspection," in *7th International Precision Assembly Seminar (IPAS)*, 2014.

[33] S. P. Javier, M.-L. Enric and G. Facciolo, "TV-L1 Optical Flow Estimation," *Image Processing On Line,* vol. 3, pp. 137-150, 2013.

[34] D. Padfield, "Masked Object Registration in the Fourier Domain," *IEEE Transactions on Image Processing,* vol. 21, no. 5, pp. 2706-2718, 2012.

[35] Z. Ren, F. Fang and N. e. a. Yan, "State of the Art in Defect Detection Based on Machine Vision," *International Journal of Precision Engineering and Manufacturing-Green Technology,* 2021.